Annals of Anatomy 222 (2019) 103–113

Contents lists available at ScienceDirect

Annals of Anatomy

journal homepage: www.elsevier.com/locate/aanat

RESEARCH ARTICLE

Ontogeny of calcium-binding proteins in the cingulate cortex of the guinea pig: The same onset but different developmental patterns

Beata Hermanowicz-Sobieraj*, Krystyna Bogus-Nowakowska, Maciej Równiak, Anna Robak*

Department of Animal Anatomy and Physiology, Faculty of Biology and Biotechnology, University of Warmia and Mazury in Olsztyn, Pl. Łódzki 3, 10-727 Olsztyn, Poland

ARTICLE INFO

Article history:
Received 25 May 2018
Received in revised form
27 November 2018
Accepted 29 November 2018

Keywords:
Cingulate cortex
Ontogeny
Calbindin
Calretinin
Parvalbumin
Guinea pig

ABSTRACT

This paper compared the density of calbindin D28k (CB), calretinin (CR) and parvalbumin (PV) containing neurons in prenatal, newborn and postnatal periods in the cingulate cortex (CC) of the guinea pig as an animal model. The distribution and co-distribution among calcium-binding proteins (CaBPs) was also investigated during the entire ontogeny. The study found that CB-positive neurons exhibited the highest density in the developing CC. The CC development in the prenatal period took place with a high level of CB and CR immunoreactivity and both of these proteins reached peak density during fetal life. The density of PV-positive neurons, in contrast to CB and CR-positive neurons, reached high levels postnatally. The observed changes of the CaBPs-positive neuron density in the developing CC coincide with developmental events in the guinea pig. E.g. the eyes opening moment may be preceded by elevated levels of CB and CR at E50, whereas high immunoreactivity of PV from P10 to P40 with a peak at P20 may indicate the participation of PV in enhancement of the inhibitory cortical pathway maturation.

1. Introduction

The cingulate cortex (CC) is one of the major components of a closed neural circuit (the Papez circuit), important for memory control and emotion expression (Papez, 1995; Vann and Nelson, 2015). The CC resides in the inner surface of the cerebral hemispheres and is usually considered to be a part of the limbic cortex. Although the CC is usually divided into different cytoarchitectural parts based on various criteria, there is common consent that anterior (ACC) and posterior (PCC) parts are the main regions of the CC in mammals. Numerous functional and anatomical data have highlighted the role of the ACC in cognitive and emotional processing (Allman et al., 2001; Etkin et al., 2011). A close relationship between ACC maturation and the ability to regulate emotion was revealed (Hung et al., 2012). Interestingly, the ACC is one of the frontal brain structures whose development continues until early adulthood (Shaw et al., 2008; Hung et al., 2012). The PCC is known to be involved in modifying behavior in response to unpredictable changes, face processing, consciousness maintenance as well as in integrating the sense of self-location (Oblak et al., 2011; Pearson et al., 2011; Zhang et al., 2017; Guterstam et al., 2015). The PCC is also important for long-term memory formation (Bird et al., 2015). Abnormalities of the CC anatomy and functional connections have been observed in a number of neuropsychiatric disorders (Foland-Ross et al., 2014; Leech and Sharp, 2014) and the CC is one of the first brain structures affected by Alzheimer's disease (Buckner et al., 2009; Raj et al., 2012). An important factor in the regulation of activities mediated by the CC is GABAergic control. For instance, differences in GABA levels in the ACC are related to fear recovery intensity in young men (Levar et al., 2017). Moreover, GABA-level reduction in the ACC is linked to the problem of recurrent depression (Gabbay et al., 2017). In the mammalian cerebral cortex, excitatory pyramidal neurons, which use glutamate as a neurotransmitter, constitute 70–80% of the total neurons, while the remaining 20–30% constitute interneurons using GABA as a major neurotransmitter (DeFelipe and Farinas, 1992; Kawaguchi and Kubota, 1997; Markram et al., 2004). GABA signaling plays a vital role in orchestrating and controlling cortical circuitry development. Depending on the period of ontogeny, GABA may act as an inhibitory or excitatory neurotransmitter (Wang et al., 2002; Dieni et al., 2012; Moss and Toni, 2013). The excitatory properties of GABA decrease gradually with differentiation of immature neurons into the mature forms (Pontes et al., 2013). Markers for examining the GABAergic system complexity in the cerebral cortex

* Corresponding authors.
E-mail addresses: beata.hermanowicz@uwm.edu.pl (B. Hermanowicz-Sobieraj), ankar@uwm.edu.pl (A. Robak).

https://doi.org/10.1016/j.aanat.2018.11.007
0940-9602/

are calcium-binding proteins (CaBPs), as the most specific among them (calbindin D28k — CB, calretinin — CR and parvalbumin — PV) co-exist with GABA in separate populations of non-pyramidal neurons. Moreover, interneurons containing CaBPs constitute 90% of total GABAergic neurons in the macaque monkey cerebral cortex, emphasizing the same essential role of calcium ions for neuronal functions (DeFelipe et al., 1989; DeFelipe, 1993; Raghanti et al., 2010). Each of these three CaBPs are notably useful neuronal markers in view of their variable localization and abundance in both developing and adult brains (Hof et al., 2001; Bogus-Nowakowska et al., 2012; Żakowski and Robak, 2013). They are suitable markers for determining developmental alterations of normal brain organization and for detecting changes in various pathological states (Żakowski and Robak, 2013; Ahmadian et al., 2015). Moreover, according to the brain region, its connections or species of animal, expression of individual CaBPs may also vary (Alonso et al., 1990; Celio, 1990). To date, no study has investigated changes in the density of neurons positive for CB, CR and PV in the CC both throughout fetal and postnatal development of the guinea pig. Most reports concern CaBP occurrence in the adult mammals (Hof and Nimchinsky, 1992; Hof et al., 1993; Nimchinsky et al., 1997; Zhao et al., 2013; Xu and Zhang, 2015; Hermanowicz-Sobieraj et al., 2018). Only a few papers relate to CB, CR and PV immunoreactivity during postnatal development in the cat, dog and rat (Alcantara et al., 1993; Alcantara and Ferrer, 1995; de Lecea et al., 1995; Schierle et al., 1997; Moon et al., 2002). Among commonly used species of rodents, the guinea pig is an intriguing laboratory animal in biomedical studies. The guinea pig appears to be more comparable to humans than to generally examined rodents, e.g. in the aspect of ontogeny (Dobbing and Sands, 1970; West, 1987; Workman et al., 2013). Therefore, in the present paper, we focus on comparing the density of CB, CR and PV-positive neurons among stages of prenatal, newborn and postnatal periods in the CC of the guinea pig. We also investigated the distribution and co-distribution of CaBPs in this brain region throughout ontogeny.

2. Material and methods

2.1. Animals

The study was conducted on 21 female Dunkin-Hartley guinea pigs (Nofer Institute Occupational Medicine in Łódź, Poland), divided according to the days of fetal and postnatal life into seven experimental groups: E40, E50, E60 — 40th, 50th, 60th day of gestation, P0 — newborn, P10, P20, P40 — 10th, 20th, 40th day after birth. In addition, data from our previously published paper (Hermanowicz-Sobieraj et al., 2018) concerning the numbers of perikarya containing CB, CR and PV in the CC of the adult guinea pig (P100) were used to analyze the statistical differences among P100 and stages examined in the present paper as well as to compare the density of neurons among all the stages. The CC of three specimens were examined in each group. The animal care and treatment procedures were performed in accordance with guidelines of the European Union Directive for animal experiments (2010/63/EU). All protocols were accepted by the Local Animal Ethics Committee of the University of Warmia and Mazury in Olsztyn, Poland. All details of tissue preparation have been described in our previously published manuscript (Hermanowicz-Sobieraj and Robak, 2017).

2.2. Immunohistochemistry

Procedures for immunostaining were consistent with those previously reported (Hermanowicz-Sobieraj and Robak, 2017). The sections containing the CC were processed for single immunoenzymatic labelling (DAB method) and double immunofluorescence labelling. For the first labelling method, the following antibodies were used in the study: rabbit anti-CB D28k (1:4000, code CB-38, Swant, Switzerland), mouse anti-CR (1:4000, code 6B3, Swant, Switzerland), mouse anti-PV (1:4000, code P3088, Sigma Aldrich, USA). For the second labelling method, two mixture solutions of antibodies were prepared: rabbit anti-CB D28k (1:4000, code CB-38, Swant, Switzerland) and mouse anti-CR (1:4000, code 6B3, Swant, Switzerland) as well as rabbit anti-CB D28k (1:4000, code CB-38, Swant, Switzerland) and mouse anti-PV (1:4000, code P3088, Sigma Aldrich, USA). In order to show the bound antibodies, sections were incubated with anti-rabbit Alexa Fluor 555 antibodies (1:800, code A-31572, Molecular Probes, USA) to visualize CB D28k and anti-mouse Alexa Fluor 488 antibodies (1:800, code A-21202, Molecular Probes, USA) to visualize CR and PV.

An Olympus BX51 microscope equipped with a CCD camera connected to a PC was used for analysis of stained sections. Images were acquired with Cell-F software (Olympus GmbH, Germany).

2.3. Controls

The specificity of the primary antibodies used in the present study were confirmed in our previous studies (Równiak et al., 2015; Hermanowicz-Sobieraj and Robak, 2017; Hermanowicz-Sobieraj et al., 2018) and by other investigators (Airaksinen et al., 1997; Zimmermann and Schwaller, 2002; Mészár et al., 2012). The specificity of the primary antibodies was also investigated by the manufacturers. Immunoblot analysis was used to test rabbit anti-CB (CB-38) and mouse anti-CR (6B3). These both antibodies showed band at 28 kDa for CB and 29 kDa for CR in immunoblots of the guinea pig brain extracts. To test the specificity of the secondary antibodies, omission of primary antibodies, their replacement by non-immune sera, PBS or irrelevant antibodies were applied. A complete lack of immunoreactive elements was detected.

2.4. Cell count and statistics

The neurons positive for CB, CR and PV were counted on sections containing the CC throughout the rostrocaudal extent with the use of an Olympus BX51 microscope equipped with Cell-F image analysis software (Olympus GmbH, Germany) in subsequent stages of development. The same number of sections per animal (n = 3) were always analyzed depending on the period of development. Every 7th, 12th and 16th section was examined in fetal, newborn and postnatal brains, respectively. For each tested brain, the starting and ending points were always constant. In order to differentiate layers in the guinea pig CC, sections stained by the Klüver-Barrera method were used (Robak et al., 2003). The number of labeled neurons was counted at 40× magnification using the 347.6 μm × 260.7 μm field as test frames, which covered the entire examined brain region per section. To calculate the mean density of neurons within the whole CC at each developmental stage, the number of CB, CR and PV-positive neurons from test frames per section were averaged. The obtained neural number was then averaged on all examined sections per brain and subsequently averaged at each developmental stage. Mean neural density refers to the test frame area and the obtained results were expressed as the number of neurons/mm^2. To determine the mean density of neurons at P100, we recalculated our previously published results concerning the number of perikarya containing CB, CR and PV in the CC of an adult guinea pig (Hermanowicz-Sobieraj et al., 2018). The analysis of statistical differences among developmental stages (E40, E50, E60, P0, P10, P20, P40, P100) was performed using one-way ANOVA and Tukey's post hoc t-test ($^*P \leq 0{,}05$; $^{**}P \leq 0{,}001$).

3. Results

The immunohistochemical analysis revealed the presence of cell populations and fibers positive for CB, CR and PV in the CC of the guinea pig throughout ontogeny. All examined CaBPs showed immunoreactivity at E40 and they were present in all studied stages. The CB-positive neuron density was the highest in the CC in most of studied stages. The density of PV-positive neurons was the least numerous in the CC at early prenatal developmental stages, while their density later increased. Contrary to PV, the density of CR-positive neurons at early fetal stages was high and it then decreased. The density of CB, CR and PV-positive neurons in the CC in subsequent developmental stages is shown in Figs. 1 and 7.

3.1. Calbindin

Among the three studied proteins, the CB-positive neurons showed the highest density and were observed in the CC from E40 onwards. Although all layers of the CC contained CB-positive structures, only single-CB containing cells were noted in layer I, while the remaining CC layers were characterized by high CB immunoreactivity in both perikarya and fibers. In general, CB-positive cells in the V–VI layers of the CC were intensely stained and loosely arranged in comparison with the perikarya in layers II–III, which were placed close together and displayed rather low immunoreactivity (Fig. 2A). CB containing fibers within the layers V–VI were varicose and oriented in different directions, while in layers II–III the fibers were smooth and mostly oriented in parallel to the corpus callosum fibers (Fig. 5A–B). In general, perikarya and fibers positive for CB were similarly distributed within the CC layers throughout ontogeny, although their delineation was more clearly observed after E50. The density of CB-positive neurons decreased throughout the CC ontogeny (Figs. 1 A, 2 B–H, 7). The highest density of neurons positive for this protein was detected at E40. In two subsequent developmental stages, the CB-positive neuron density rapidly decreased (**P < 0,001). The first decline was observed at E50 (**P < 0,001) and the second decline at E60 (**P < 0,001). The decline between E40 and E50 was lower than between E50 and E60 (Fig. 1A). From E60 to P10 the density was maintained at a similar level (P > 0.05), while at P20 it decreased (**P < 0.001) and remained unchanged to P40 (P > 0.05) (Fig. 1A). At P100, another significant decrease of the CB-positive neuron density was noted (**P < 0.001) (Fig. 1A). Therefore, the density of neurons at P100 differs significantly from all other stages examined (Fig. 1A). The decline in CB-positive neuron density in postnatal developmental stages was lower than during prenatal development. CB-positive neurons co-localized sporadically with PV from E50 onwards (Fig. 6A–B), but never contained CR in the CC throughout ontogeny (Fig. 6C–D).

3.2. Calretinin

CR was present within the CC of the guinea pig in all developmental stages in perikarya and fibers. Two subpopulations of neurons positive for CR were observed (with higher and lower immunoreactivity). Varicose and smooth fibers oriented in different directions transversing the CC were detected among CR-positive perikarya (Fig. 5C–D). The distribution pattern of CR-positive structures was similar in subsequent age groups. In the layer I of the CC, CR containing cells were rarely noted. In general, the vast majority of CR-positive perikarya was observed in the layers II–III of the CC (Figs. 3 A, 7). Significant differences in the density of CR-positive neurons were found among studied developmental stages in the CC (Figs. 1 B, 3 B–H, 7). The density of CR-positive neurons was relatively high at E40 and significantly increased up to E50 (**P < 0.001), reaching peak value at this stage. At E60, an abrupt decrease was noted (**P < 0.001) (Fig. 1B) and, from this

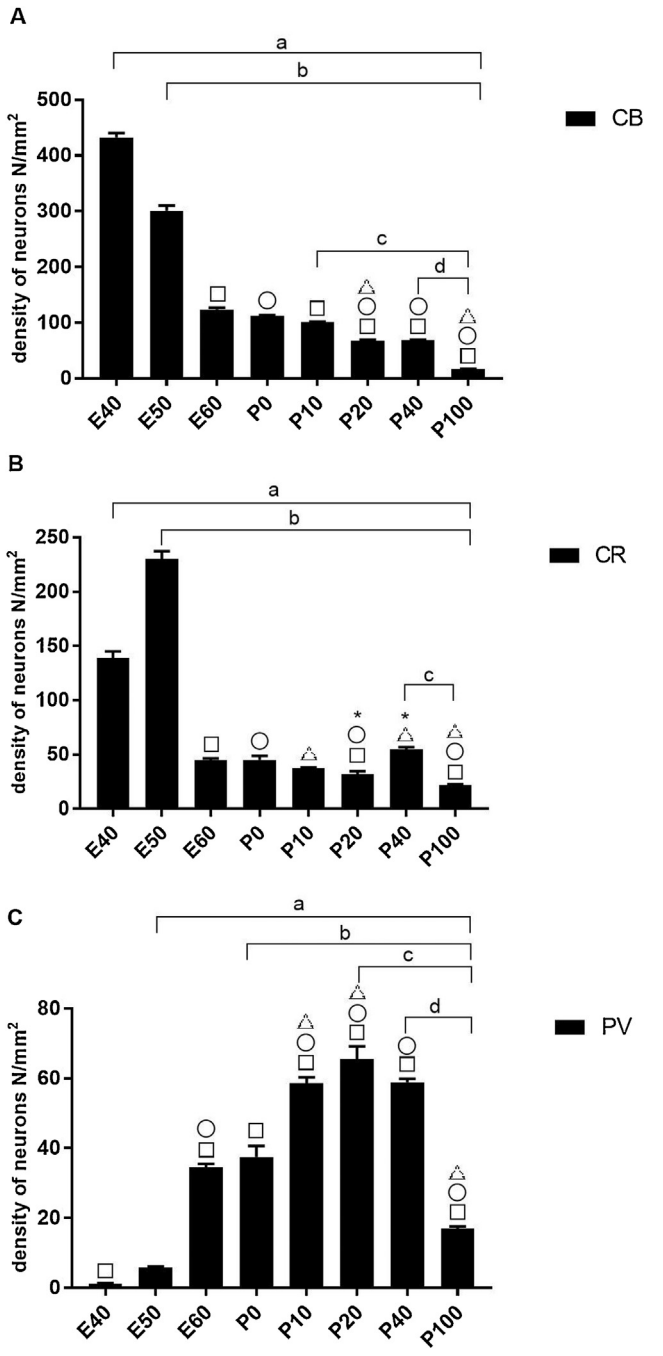

Fig 1. The CB (A), CR (B) and PV (C) — positive neuron density in the guinea pig CC at fetal (E40, E50, E60), newborn (P0) and postnatal (P10, P20, P40, P100) developmental stages. Data were statistically evaluated by one-way ANOVA and Tukey's post hoc t-test (differences among stages) (*P ≤ 0,05; **P ≤ 0,001).
A: (a) — E40 differs from all other developmental stages (**P < 0,001), (b) — E50 differs from all other developmental stages (**P < 0,001), (c) — P10 differs from P20–P100 (**P < 0,001), (d) — P40 differs from P100 (**P < 0,001); □ — E60 differs from P10–P100 (**P < 0,001), ○ — P0 differs from P20–P100 (**P < 0,001), △ — P20 differs from P100 (**P < 0,001).
B: (a) — E40 differs from all other developmental stages (**P < 0,001), (b) — E50 differs from all other developmental stages (**P < 0,001), (c) — P40 differs from P100 (**P < 0,001); □ — E60 differs from P20 (*P < 0,05) and P100 (**P < 0,001); ○ — P0 differs from P20 (*P < 0,05) and P100 (**P < 0,001); △ — P10 differs from P40 (*P < 0,05) and P100 (**P < 0,001); * — P20 differs from P40 (**P < 0,001).
C: (a) — E50 differs from E60–P100 (**P < 0,001), (b) — P0 differs from P10–P100 (**P < 0,001), (c) — P20 differs from P40 (*P < 0,05) and P100 (**P < 0,001), (d) — P40 differs from P100 (**P < 0,001); □ – E40 differs from E60–P100 (**P < 0,001), ○ — E60 differs from P10–P100 (**P < 0,001); △ — P10 differs from P20 (*P < 0,05) and P100 (**P < 0,001).

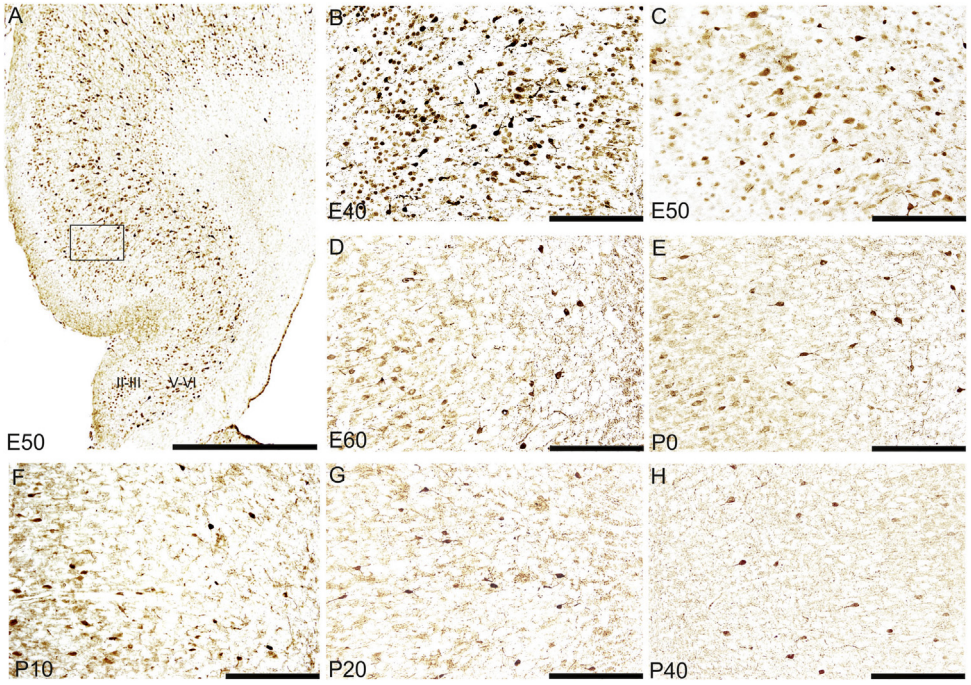

Fig. 2. CB immunoreactivity in the guinea pig CC (A–H); distribution pattern of CB-positive structures throughout the whole CC (A); CB-positive structures at fetal (B–D), newborn (E) and postnatal (F–H) developmental stages. II–III — the CC superficial layers, V–VI — the CC deep layers. Scale bars: 1000 μm (A), 200 μm (B–H); note the frame at image A, it shows the region from which enlarged images (B—H) were taken.

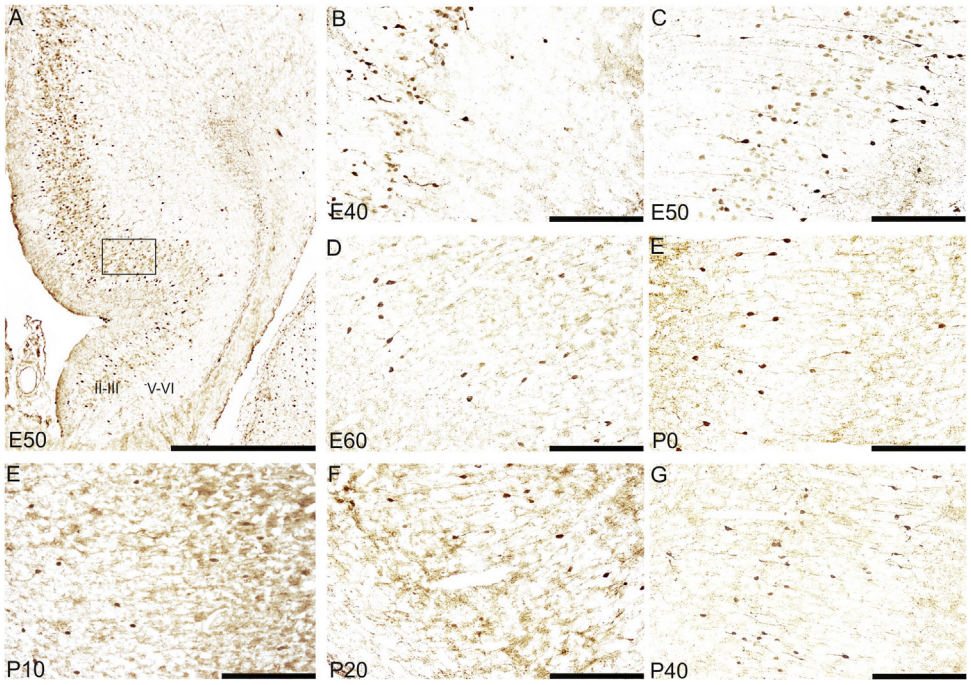

Fig. 3. CR immunoreactivity in the guinea pig CC (A–H); distribution pattern of CR-positive structures throughout the whole CC (A); CR-positive structures at fetal (B–D), newborn (E) and postnatal (F–H) developmental stages. II–III — the CC superficial layers, V–VI — the CC deep layers. Scale bars: 1000 μm (A), 200 μm (B–H); note the frame at image A, it shows the region from which enlarged images (B–H) were taken.

stage, the density of CR-positive neurons remained at a similar level until P20, so that from E60 to P20 the density of CR-positive neurons did not differ significantly. At P40 a slight, but statistically significant, increase of the CR-positive neuron density was reported (**$P < 0.001$) (Fig. 1B), while at P100 a decrease of the density was noted (**$P < 0.001$) and the density of neurons at P100 differs significantly from all other stages examined (Fig. 1B). During the CC development, no co-localization between CR and CB was detected (Fig. 6C–D).

3.3. Parvalbumin

Both perikarya and fibers that displayed immunoreactivity for PV were found in the CC at all studied developmental stages, from E40 onwards. The fibers, usually oriented in different directions, could be divided into two types based on their morphology: smooth and varicose (Fig. 5E–F). PV-positive structures were restricted to the layers V–VI of the CC at E40, while at E50, single perikarya containing this protein also appeared in the layers II–III (Fig. 7).

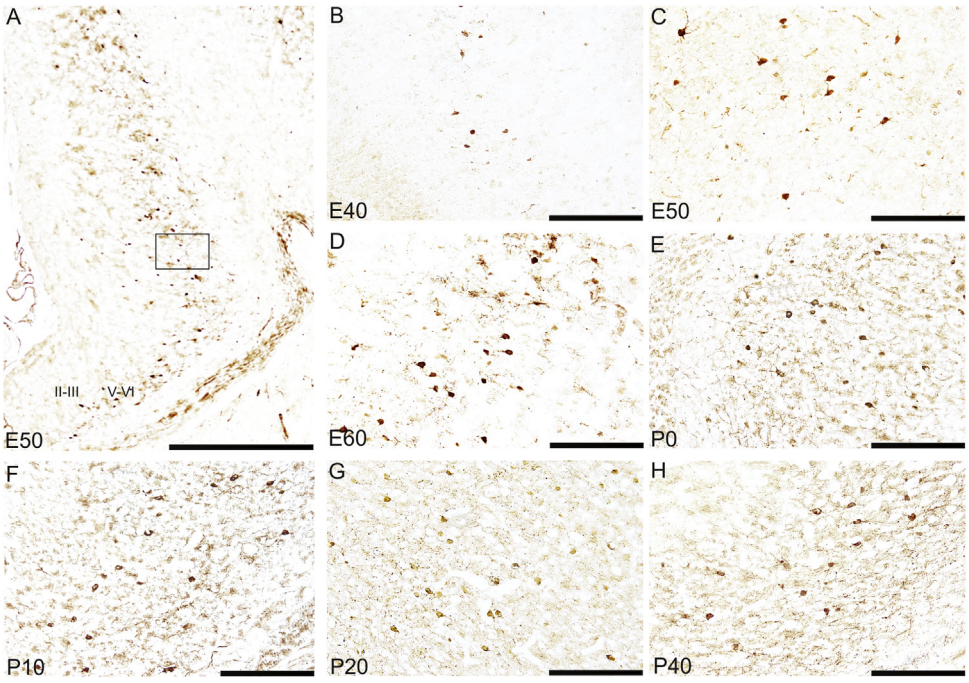

Fig. 4. PV immunoreactivity in the guinea pig CC (A–H); distribution pattern of PV-positive structures throughout the whole CC (A); PV-positive structures at fetal (B–D), newborn (E) and postnatal (F–H) developmental stages. II–III — the CC superficial layers, V–VI — the CC deep layers. Scale bars: 1000 μm (A), 200 μm (B–H); note the frame at image A, it shows the region from which enlarged images (B–H) were taken.

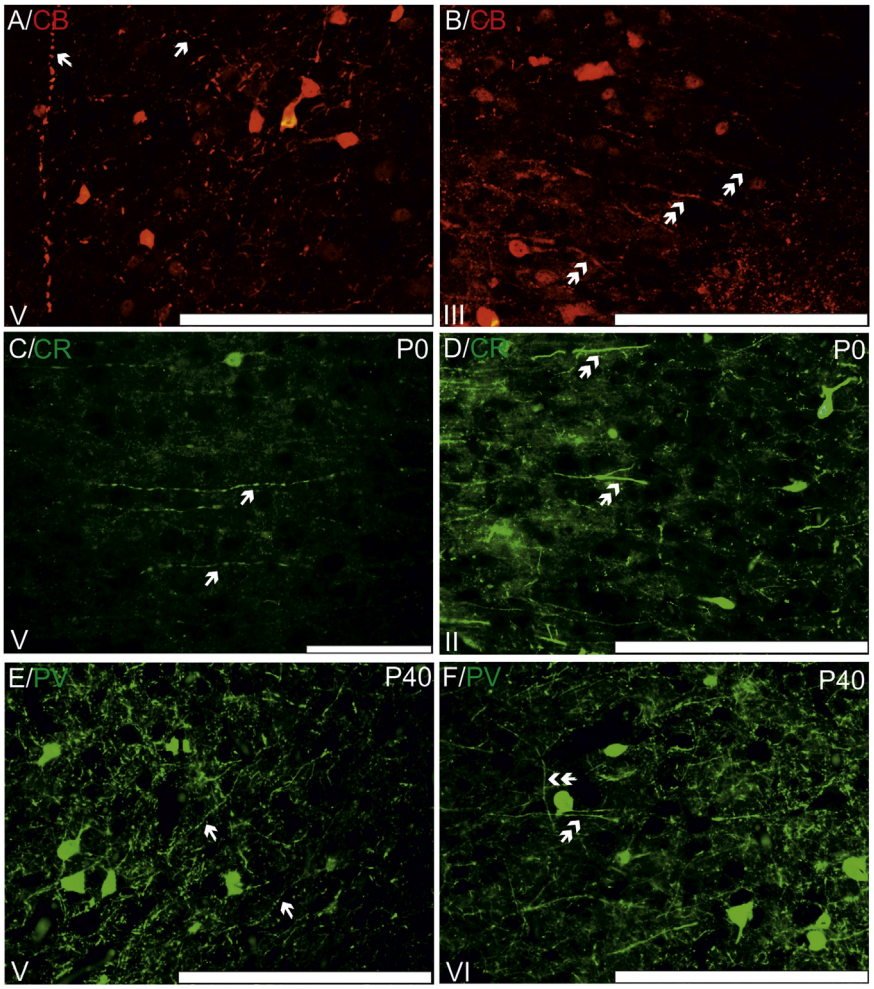

Fig. 5. CaBPs immunoreactivity in the fibers of the guinea pig CC. Note varicose (single arrows) and smooth (double arrows) immunoreactive fibers for CB (A, B), CR (C, D) and for PV (E, F); roman numerals indicate layers of the CC. Scale bars: 200 μm (A, B, D–F), 100 μm (C).

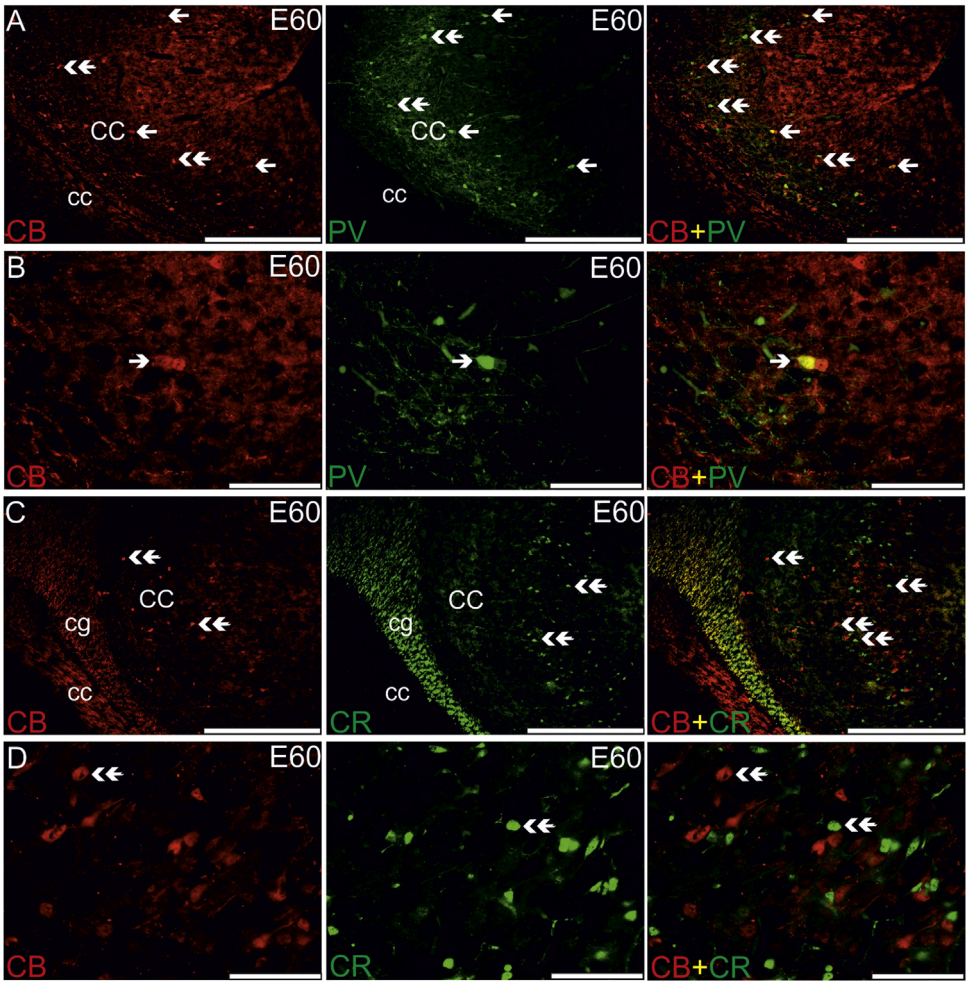

Fig. 6. Co-localization patterns of CaBPs in the guinea pig CC. Co-localization of CB and PV (A, B); lack of co-localization of CB and CR (C, D) in the guinea pig CC. Note co-localization of CB and CR in the cg. Single arrows indicate double labelled cells; double arrows indicate single labelled cells; cg — cingulum; cc — corpus callosum. Scale bars: 500 μm (A, C), 100 μm (B, D).

In subsequent developmental stages, the pattern of PV distribution was almost unchanged. In particular, PV-positive perikarya were present in all layers of the CC with the exception of layer I. They were more numerous in layers V–VI of the CC than in layers II–III (Figs. 4 A, 7). The density of PV-positive neurons in the CC varied considerably throughout development (Figs. 1 C, 4 B–H, 7). At E40 and E50, the PV-positive neuron density was low and it considerably increased at E60 (**$P < 0.001$) and remained at a similar level until P0 ($P > 0.05$) (Fig. 1C). From P0, the density of PV-positive neurons increased up to P10 (**$P < 0.001$) and remained high up to P40. However, a slight increase was noted at P20 (*$P < 0.05$) and the PV-positive neuron density reached the highest value at this stage. From P40, the density of PV-positive neurons slightly decreased in relation to P20 (*$P < 0.05$), while the largest decrease was noted at P100 (**$P < 0.001$) (Fig. 1C). Discrete co-localization between PV and CB in neurons of the CC was observed after E50 (Fig. 6A–B).

4. Discussion

To the extent of our knowledge, the present study is the first to examine the developmental changes of three principal markers for GABAergic cortical neurons (CB, CR and PV) in the guinea pig CC. The density of CaBPs-positive neurons differs greatly among developmental stages. Our results show that among the three examined CaBPs, the CB-positive neuron density is the highest during the CC development. The densities of both CB and CR-positive neurons reach peak values during fetal development. Elevated levels of CB and CR at fetal stages, especially at E50, are essential for guinea pig CC prenatal development. The PV-positive neuron density, contrary to CB and CR, reaches a high level postnatally in the period from P10 to P40 with the peak value at P20.

4.1. CB, CR and PV immunoreactivity in the CC — interspecies comparisons

Based on the available data, it can be concluded that the expression patterns of CaBPs are rather analogous among different mammalian species during corticogenesis. Namely, CB and CR usually start to be observed in the developing cortical plate, and although PV occurs in a later period of ontogeny, it usually appears when cortical lamination is practically completed (Hof et al., 1999). In the guinea pig, these three CaBPs were present in the CC in the same period of prenatal development (E40), which is not entirely consistent with the above assumption. Considering that the appearance of PV may indicate the completion of the cortical lamination, it might be assumed that the CC lamination in the guinea pig is practically completed at E40. In the guinea pig CC, five cortical layers were distinguished: three superficial layers (I–III) and two deep layers (V–VI). According to Wree et al. (1981), there is a lack of layer IV in the guinea pig CC. The CC neurogenesis in the rat occurs in the period between E13 and E20, which approximately corresponds to the period between E23 and E34 in the guinea pig (Bayer, 1990;

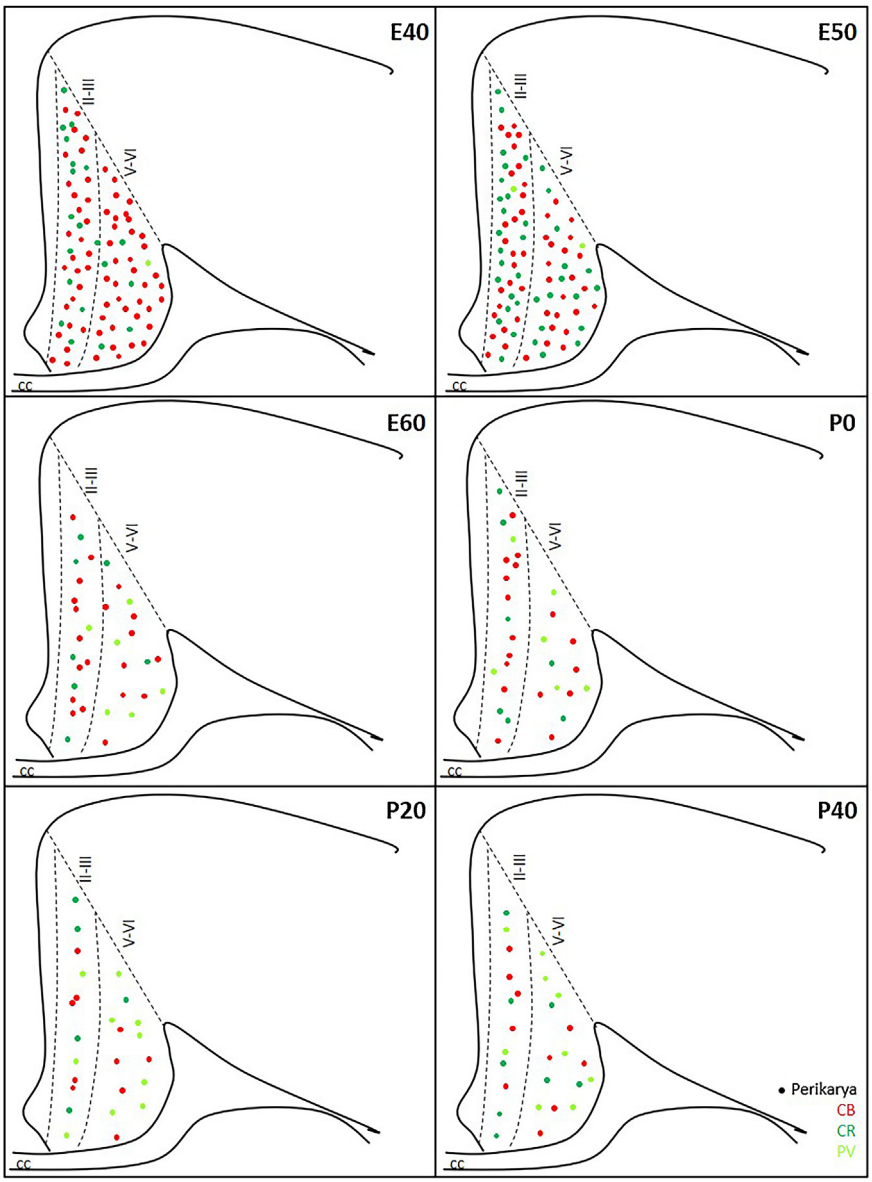

Fig. 7. Schematic drawing showing the distribution of CB, CR and PV-positive perikarya throughout the CC guinea pig layers (II–III, V–VI) at fetal (E40, E50, E60), newborn (P0) and postnatal developmental stages (P20, P40).

Workman et al., 2013). The guinea pig, compared to widely-used laboratory animals, is an unusual rodent, which in many aspects more resembles humans. Namely, in the guinea pig and humans, in contrast to the rat and mouse, dynamic brain development occurs to a large extent before the birth (Dobbing and Sands, 1970; West, 1987). In the guinea pig brain development, three trimesters occurring prenatally were distinguished, which is more complementary to human brain development. In the rat and mouse, one of the three trimesters occurs after birth (West, 1987). Interestingly, during the prenatal period, the GABAergic action switches from stimulating to inhibitory in a group of mammals, which have relatively long gestation, including humans and the guinea pig, although in other rodents operation of the GABAergic system remains stimulating during postnatal life (Coleman et al., 2013; Shaw et al., 2018).

Some changes in CaBPs immunoreactivity during the guinea pig CC development seem to correspond more to those demonstrated in the cat than in the dog and rat. In the cat, the density of CB-positive neurons in the CC generally decreased in the period from P0 to P28/35 (Alcantara and Ferrer, 1995). A similar decrease was observed in the guinea pig in the period from E40 to E60, which corresponds approximately to the examined postnatal period (P0-P28/35) in the cat (Workman et al., 2013). On the other hand, CB immunoreactivity in the dog, in contrast to the guinea pig, increased in non-pyramidal cells of the ACC from P0 to P28 and then gradually decreased to P180 (Moon et al., 2002). As regards PV, in the dog and rat, in contrast to the guinea pig, the first neurons containing this protein were observed in the CC at P7 and P8-P9, respectively (Alcantara et al., 1993; de Lecea et al., 1995; Moon et al., 2002). In the guinea pig, PV immunoreactivity was observed from E40. Taking into account that P8-9 in the rat coincides to E47-E48 in the guinea pig (Workman et al., 2013), we may assume that PV in the guinea pig appears earlier than in the rat. Despite the fact that PV appeared in different periods of the CC ontogeny in various mammals (interspecies differences), immunoreactivity of this protein changed in a similar way during postnatal development. In the dog ACC (Moon et al., 2002), PV immunoreactivity during postnatal development initially increased and then gradually decreased, which seems to reflect

the postnatal changes in the density of PV-positive neurons in the guinea pig.

4.2. CB, CR and PV immunoreactivity in the CC — functional implications

GABAergic neurons might be segregated into distinct non-overlapping subgroups based on their CaBPs expression: CB, CR and PV in the cerebral cortex. Although GABAergic interneurons represent a considerable minority among total mammalian cortical neurons, their role in general activity modulation of the cerebral cortex is fundamental. CB, CR and PV, as appropriate markers for examining the architecture of interneuron networks in the cerebral cortex, belong to morphologically and functionally distinct subpopulations of GABAergic interneurons. A majority of CB-positive interneurons have a morphology of double-bouquet, while CR-positive interneurons (apart from double-bouquet cells) are expressed by bipolar and Cajal–Retzius cells (DeFelipe et al., 1990; Conde et al., 1994; Wouterlood et al., 2000). Both CB and CR-positive interneurons make synapses on dendrites of pyramidal neurons and are classified as non-fast-spiking (Zaitsev et al., 2005). On the other hand, PV is expressed in basket and chandelier populations of GABAergic neurons (Kawaguchi and Kubota, 1997; Kawaguchi and Kondo, 2002). These types of interneurons exhibit characteristics of fast-spiking cells, although their electrophysiological properties are not the same (Woodruff et al., 2009). Fast-spiking PV interneurons are essential for signal transmissions in neocortical microcircuits (Sohal et al., 2009). They induce gamma oscillations, which are recorded in cortical regions during the performance of cognitive operations, including memory tasks (Gulyás et al., 2010). GABAergic signaling is essential for the regulation of brain activity during development, while GABAergic transmission is disrupted in some neurodevelopmental disorders (Chattopadhyaya and Cristo, 2012). Taking into account the important role of GABA in brain development and the fact that each of the studied CaBPs mostly co-localized with GABA in the cerebral cortex, it seems acceptable that some changes of the CaBPs expression at various periods of the CC development might be under GABAergic control.

The present results reported that the density of CB-positive neurons in the CC was the highest at E40 and after this time decreased until P100. More significant declines in the CB-positive neuron density were observed during fetal life than in newborns and after birth, however, the most considerable decrease was identified between E50 and E60. Interestingly, in the same period, a rapid decline of the CR-positive neuron density was observed in the guinea pig CC. This reduction may be linked to the action of the GABAergic system, which switches from stimulating to inhibitory at E55 in the guinea pig hippocampus (Coleman et al., 2013). This switch may be triggered by maternal oxytocin during labor, thus providing protection against anoxic injury in the fetal brain (Carbillon, 2007). In various brain regions, the reduction of CB immunoreactivity coincides with the appearance of PV. A similar relationship was observed in the guinea pig CC. Namely, a sharp decrease of the CB-positive neuron density between E50 and E60 seems to coincide with a rapid increase in the PV-positive neuron density. Moreover, a period of co-existence between CB and PV might also precede the reduction of CB expression (Yan et al., 1995; Alcantara et al., 1996). On the other hand, according to Legaz et al. (2005) neurons containing CB may express PV, without CB loss. Co-localization of CB and PV in the guinea pig may suggest collaboration of these two CaBPs throughout the CC ontogeny. CB acting as Ca^{2+} buffer and/or sensor (Schwaller et al., 1997; Berggård et al., 2002) might compensate PV, thus ensuring proper Ca^{2+} level in the CC developing neurons. The process of neuronal development is particularly vulnerable to a loss of Ca^{2+}, which is directly related to increased apoptosis (Turner et al., 2007). CB is known for its unique anti-apoptotic properties which are due, not only to Ca^{2+} buffering, but also the ability to cooperate with caspase-3 and inhibit its pro-apoptotic activity (Bellido et al., 2000). The cooperation between CB and caspase-3 is dependent on the Ca^{2+} level bound to CB (Bobay et al., 2012). As CB was the most expressed CaBPs within the CC almost throughout the entire developmental period, it can be assumed that CB creates the crucial anti-apoptotic Ca^{2+} buffering system during the guinea pig CC development. It should be also pointed out that in adult brain CB/PV neurons also exist and they are believed to be basket-like neurons which provide a strong perisomatic inhibition of local pyramidal neurons (Pitkänen and Amaral, 1993; Sorvari et al., 1995; Woodruff and Sah, 2007). However, it should be kept in mind that the level of the co-expression to be region, age and species-dependent (Alcantara et al., 1996; Mascagni et al., 2009). E.g. in the adult rat cortex, CB and PV were present in non-overlapping populations of GABAergic interneurons, however double-labelled cells were found in all cortical layers between P9 and P21, coinciding with the onset of parvalbumin expression (Alcantara et al., 1996).

In the guinea pig CC development, the density of CR-positive neurons reached the highest level at E50 and abruptly declined at E60. It should be noted that the CB-positive neuron density at E50 is also high (higher than CR). The high level of CR and CB density at E50 in the CC may be related to events which occur in this period in the development of the guinea pig, i.e. eyes opening. The moment of eyes opening in the guinea pig occurs at E52 (Workman et al., 2013). Interestingly, activation of the ACC in visual attention was revealed (Wu et al., 2017). Moreover, depending on whether the eyes are open or not, effective connectivity between ACC and PCC changes (Piantoni et al., 2013). It seems quite possible that the moment of eyes opening is preceded by an increase of CR immunoreactivity in the CC. It seems to be noteworthy that after reduction of the CR-positive neuron density at E60 and a generally similar density from E60 to P20, an increase in the density of CR-positive neurons at P40 was documented. Thus, it might be considered that down-regulation of PV immunoreactivity observed at P40 in the guinea pig CC allows the upregulation of CR immunoreactivity in the CC in the same time. In the guinea pig life, P40 corresponds to adolescence and an increase in CR immunoreactivity may be related to this developmental period during ontogeny. During adolescence, a reduced level of GABA in the ACC was noted. This reduced GABA level contributes to the reduction of ability to inhibit risky behaviors among adolescents (Silveri et al., 2013). It is worth noting that the inhibitory GABAergic neurotransmission in the immature frontal cortex is only started (Silveri et al., 2013). Among frontal brain regions, the ACC is one of the last whose development lasts till early adulthood (Shaw et al., 2008; Hung et al., 2012). Moreover, adolescence is the time when the first symptoms of some neurodevelopmental diseases, such as schizophrenia, may appear (Gogtay et al., 2011). Taking into account that some anatomical anomalies in the ACC in schizophrenia has been observed (Fornito et al., 2009) and the CR expression does not differ between patients with schizophrenia and healthy control subjects (Brisch et al., 2015), it is quite likely that an increase in CR immunoreactivity at P40 in the CC may be the factor that confers the resistance of neurons vulnerable to degeneration in schizophrenia in further stages of development. However, although CB is the main Ca^{2+} buffer in the developing CC, the role of CR is equally important in the period from E40 to E60, especially so since CR, like CB, may act as both a Ca^{2+} buffer and sensor (Billing-Marczak and Kuźnicki, 1999). The CR-positive neuron density was higher than the PV-positive neuron density in fetal stages. In the development of the guinea pig CC, a low density of neurons positive for PV were noted from E40 and the density increased considerably between E50 and E60. The presence of PV in the guinea pig CC at E40 may coincide with initiation of GABAergic synaptic transmission. GABAergic inhibitory synaptic

responses were registered in the mouse neocortex after E18, which correspond to E34 in the guinea pig (Verhage et al., 2000; Workman et al., 2013). However, it should be noted that, early in development, GABA is excitatory and in the guinea pig hippocampus it switches to being inhibitory around E55 (Coleman et al., 2013). Thus, the increase in PV density noted at E60 in the guinea pig CC goes along with the switch of the role of GABA from excitation to inhibition (Coleman et al., 2013). The effectiveness of GABAergic synaptic responses might be modulated by brain-derived neurotrophic factor, which takes part in the neuronal laminas forming in the developing cerebral cortex (Fukumitsu et al., 2006). PV is involved in the maturation of inhibitory cortical circuits (Alcantara et al., 1993). The high level of the PV-positive neuron density in the CC was identified from P10 to P40 with the peak noted at P20. This may be associated with enhancement of the inhibitory cortical circuit maturation in response to mother separation from young guinea pigs. Around P20, a guinea pig is usually weaned from its mother. Mother separation is a potentially stressful situation in the guinea pig's life. The guinea pig is a precocial mammal which, from the moment of birth to weaning, follows its mother and is close to her (Wewers et al., 2003). Moreover, a subset of neuronal progenitors in the guinea pig lateral striatum which at the moment of birth were quiescent, became activate during postnatal life, reaching the peak at weaning (Luzzati et al., 2014). PV is the GABAergic system component, thus alterations in PV expression might disrupt normal inhibitory neurotransmission (Miettinen et al., 1993). Interestingly, the PV-positive neuron density declined slightly between P20 and P40 and abruptly between P40 and P100 in the guinea pig CC. A similar decrease was documented in relation to a neuronal population containing doublecortin (DCX). Namely, DCX expression decreased in the guinea pig cerebral cortex from juvenile to adult stages (Xiong et al., 2008). DCX is essential for the migration of immature neurons during brain development, but it also exists in the adult brain, including the guinea pig. Both immature and migrating cells containing DCX may undergo differentiation to functional populations of GABAergic interneurons (Cai et al., 2009). As the co-localization of PV and DCX in cortical neurons was detected (Cai et al., 2009), it might be assumed that PV co-operates with DCX, thus ensuring the proper postnatal development of the guinea pig CC neurons.

5. Conclusions

In conclusion, our results revealed that the spatiotemporal expression of each CaBPs in the developing CC differs greatly. CB is a crucial Ca^{2+} buffer almost throughout the entire period of CC development. CR appears to be more essential during fetal life, while PV is more essential in the postnatal developmental period. Crucial changes in the density of neurons containing the examined CaBPs in the developing CC seem to correspond with critical events occurring in the development of the guinea pig, e.g. the elevated levels of CR and CB at E50 may precede the eyes opening moment, while a rapid decrease in CR and CB densities between E50 and E60 and a considerable increase in PV density in this period may be linked to the switch of excitatory GABA signaling to inhibitory. In turn, high PV immunoreactivity, from P10 to P40, may prove the involvement of this protein in reinforcement of the inhibitory pathway maturation in response to some stressful moments occurring in young guinea pigs, e.g. weaning from the mother.

Acknowledgements

This work was funded by grant number 12.620.031-300 UWM Olsztyn, Poland.

References

Ahmadian, S.S., Rezvanian, A., Peterson, M., Weintraub, S., Bigio, E.H., Mesulam, M.M., Geula, C., 2015. Loss of calbindin-D28 K is associated with the full range of tangle pathology within basal forebrain cholinergic neurons in Alzheimer's disease. Neurobiol. Aging 36 (12), 3163–3170.

Airaksinen, M.S., Eilers, J., Garaschuk, O., Thoenen, H., Konnerth, A., Meyer, M., 1997. Ataxia and altered dendritic calcium signaling in mice carrying a targeted null mutation of the calbindin D28k gene. Proc. Natl. Acad. Sci. U. S. A. 94 (4), 1488–1493.

Alcantara, S., de Lecea, L., Del Rio, J.A., Ferrer, I., Soriano, E., 1996. Transient colocalization of parvalbumin and calbindin D28k in the postnatal cerebral cortex: evidence for a phenotypic shift in developing nonpyramidal neurons. Eur. J. Neurosci. 8 (7), 1329–1339.

Alcantara, S., Ferrer, I., 1995. Postnatal development of calbindin D-28k immunoreactivity in the cerebral cortex of the cat. Anat. Embryol. 192 (4), 369–384.

Alcantara, S., Ferrer, I., Soriano, E., 1993. Postnatal development of parvalbumin and calbindin D28k immunoreactivities in the cerebral cortex of the rat. Anat. Embryol. (Berl.) 188 (1), 63–73.

Allman, J.M., Hakeem, A., Erwin, J.M., Nimchinsky, E., Hof, P., 2001. The anterior cingulate cortex. The evolution of an interface between emotion and cognition. Ann. N. Y. Acad. Sci. 935, 107–117.

Alonso, J.R., Coveñas, R., Lara, J., Aijón, J., 1990. Distribution of parvalbumin immunoreactivity in the rat septal area. Brain Res. Bull. 24 (1), 41–48.

Bayer, S.A., 1990. Neurogenetic patterns in the medial limbic cortex of the rat related to anatomical connections with the thalamus and striatum. Exp. Neurol. 107 (2), 132–142.

Bellido, T., Huening, M., Raval-Pandya, M., Manolagas, S.C., Christakos, S., 2000. Calbindin-D28k is expressed in osteoblastic cells and suppresses their apoptosis by inhibiting caspase-3 activity. J. Biol. Chem. 275 (34), 26328–26332.

Berggård, T., Miron, S., Onnerfjord, P., Thulin, E., Akerfeldt, K.S., Enghild, J.J., Akke, M., Linse, S., 2002. Calbindin D28k exhibits properties characteristic of a Ca^{2+} sensor. J. Biol. Chem. 277 (19), 16662–16672.

Billing-Marczak, K., Kuźnicki, J., 1999. Calretinin—sensor or buffer—function still unclear. Pol. J. Pharmacol. 51 (2), 173–178.

Bird, C.M., Keidel, J.L., Ing, L.P., Horner, A.J., Burgfess, N., 2015. Consolidation of complex events via reinstatement in posterior cingulate cortex. J. Neurosci. 35 (43), 14426–14434.

Bobay, B.G., Stewart, A.L., Tucker, A.T., Thompson, R.J., Varney, K.M., Cavanagh, J., 2012. Structural insights into the calcium-dependent interaction between calbindin-D28k and caspase-3. FEBS Lett. 586 (20), 3582–3589.

Bogus-Nowakowska, K., Litwin, D., Robak, A., Równiak, M., Żakowski, W., Wasilewska, B., Najdzion, J., Milewski, S., 2012. Distribution of cocaine and amphetamine-regulated transcript (CART) and calcium binding proteins immunoreactivity in the preoptic area of the ram. Bull. Vet. Inst. Pulawy 56 (3), 355–360.

Brisch, R., Bielau, H., Saniotis, A., Wolf, R., Bogerts, B., Krell, D., Steiner, J., Braun, K., Krzyżanowska, M., Krzyżanowski, M., Jankowski, Z., Kaliszan, M., Bernstein, H.G., Gos, T., 2015. Calretinin and parvalbumin in schizophrenia and affective disorders: a mini-review, a perspective on the evolutionary role of calretinin in schizophrenia, and a preliminary post-mortem study of calretinin in the septal nuclei. Front. Cell. Neurosci. 9, 393, http://dx.doi.org/10.3389/fncel.2015.00393.

Buckner, R.L., Sepulcre, J., Talukdar, T., Krienen, F.M., Liu, H., Hedden, T., Andrews-Hanna, J.R., Sperling, R.A., Johnson, K.A., 2009. Cortical hubs revealed by intrinsic functional connectivity: mapping, assessment of stability, and relation to Alzheimer's disease. J. Neurosci. 29 (6), 1860–1873.

Cai, Y., Xiong, K., Chu, Y., Luo, D.W., Luo, X.G., Yuan, X.Y., Struble, R.G., Clough, R.W., Spencer, D.D., Williamson, A., Kordower, J.H., Patrylo, P.R., Yan, X.X., 2009. Doublecortin expression in adult cat and primate cerebral cortex relates to immature neurons that develop into GABAergic subgroups. Exp. Neurol. 216 (2), 342–356.

Carbillon, L., 2007. Comment on "Maternal oxytocin triggers a transient inhibitory switch in GABA signaling in the fetal brain during delivery". Science 317 (5835), 197, http://dx.doi.org/10.1126/science.1141090.

Celio, M.R., 1990. Calbindin D-28k and parvalbumin in the rat nervous system. Neuroscience 35 (2), 375–475.

Chattopadhyaya, B., Cristo, G.D., 2012. GABAergic circuit dysfunctions in neurodevelopmental disorders. Front. Psychiatry 3, 51, http://dx.doi.org/10.3389/fpsyt.2012.00051.

Coleman, H., Hirst, J.J., Parkington, H.C., 2013. The GABAA excitatory-to-inhibitory switch in the hippocampus of perinatal guinea-pigs. The 40th Annual Meeting Fetal and Neonatal Physiological Society, Chile, p. 83.

Conde, F., Lund, J.S., Jacobowitz, D.M., Baimbridge, K.G., Lewis, D.A., 1994. Local circuit neurons immunoreactive for calretinin, calbindin D-28k or parvalbumin in monkey prefrontal cortex: distribution and morphology. J. Comp. Neurol. 341 (1), 95–116.

de Lecea, L., del Río, J.A., Soriano, E., 1995. Developmental expression of parvalbumin mRNA in the cerebral cortex and hippocampus of the rat. Brain Res. Mol. Brain Res. 32 (1), 1–13.

DeFelipe, J., 1993. Neocortical neuronal diversity: chemical heterogeneity revealed by colocalization studies of classic neurotransmitters, neuropeptides, calcium-binding proteins, and cell surface molecules. Cereb. Cortex 3 (4), 273–289.

DeFelipe, J., Farinas, I., 1992. The pyramidal neuron of the cerebral cortex: morphological and chemical characteristics of the synaptic inputs. Prog. Neurobiol. 39 (6), 563–607.

DeFelipe, J., Hendry, S.H., Hashikawa, T., Molinari, M., Jones, E.G., 1990. A microcolumnar structure of monkey cerebral cortex revealed by immunocytochemical studies of double bouquet cell axons. Neuroscience 37 (3), 655–673.
DeFelipe, J., Hendry, S.H., Jones, E.G., 1989. Synapses of double bouquet cells in monkey cerebral cortex visualized by calbindin immunoreactivity. Brain Res. 503 (1), 49–54.
Dieni, C.V., Chancey, J.H., Overstreet-Wadiche, L.S., 2012. Dynamic functions of GABA signaling during granule cell maturation. Front. Neural Circuits 6, 113, http://dx.doi.org/10.3389/fncir.2012.00113.
Dobbing, J., Sands, J., 1970. Growth and development of the brain and spinal cord of the guinea pig. Brain Res. 17 (1), 115–123.
Etkin, A., Egner, T., Kalisch, R., 2011. Emotional processing in anterior cingulate cortex and medial prefrontal cortex. Trends Cogn. Sci. 15 (2), 85–93.
Foland-Ross, L.C., Hamilton, P., Sacchet, M.D., Furman, D.J., Sherdell, L., Gotlib, I.H., 2014. Activation of the medial prefrontal and posterior cingulate cortex during encoding of negative material predicts symptom worsening in major depression. Neuroreport 25 (5), 324–329.
Fornito, A., Yücel, M., Dean, B., Wood, S.J., Pantelis, C., 2009. Anatomical abnormalities of the anterior cingulate cortex in schizophrenia: bridging the gap between neuroimaging and neuropathology. Schizophr. Bull. 35 (5), 973–993.
Fukumitsu, H., Ohtsuka, M., Murai, R., Nakamura, H., Itoh, K., Furukawa, S., 2006. Brain-derived neurotrophic factor participates in determination of neuronal laminar fate in the developing mouse cerebral cortex. J. Neurosci. 26 (51), 13218–13230.
Gabbay, V., Bradley, K.A., Mao, X., Ostrover, R., Kang, G., Shungu, D.C., 2017. Anterior cingulate cortex γ-aminobutyric acid deficits in youth with depression. Transl. Psychiatry 7 (8), e1216, http://dx.doi.org/10.1038/tp.2017.187.
Gogtay, N., Vyas, N.S., Testa, R., Wood, S.J., Pantelis, C., 2011. Age of onset of schizophrenia: perspectives from structural neuroimaging studies. Schizophr. Bull. 37 (3), 504–513.
Gulyás, A.I., Szabó, G.G., Ulbert, I., Holderith, N., Monyer, H., Erdélyi, F., Szabó, G., Freund, T.F., Hájos, N., 2010. Parvalbumin-containing fast-spiking basket cells generate the field potential oscillations induced by cholinergic receptor activation in the hippocampus. J. Neurosci. 30 (45), 15134–15145.
Guterstam, A., Björnsdotter, M., Gentile, G., Ehrsson, H.H., 2015. Posterior cingulate cortex integrates the senses of self-location and body ownership. Curr. Biol. 25 (11), 1416–14125.
Hermanowicz-Sobieraj, B., Bogus-Nowakowska, K., Robak, A., 2018. Calcium-binding proteins expression in the septum and cingulate cortex of the adult guinea pig. Ann. Anat. 215, 30–39.
Hermanowicz-Sobieraj, B., Robak, A., 2017. The ontogenetic development of neurons containing calcium-binding proteins in the septum of the guinea pig: late onset of parvalbumin immunoreactivity versus calbindin and calretinin. J. Chem. Neuroanat. 79, 22–31.
Hof, P.R., Glezer, I.I., Condé, F., Flagg, R.A., Rubin, M.B., Nimchinsky, E.A., Vogt Weisenhorn, D.M., 1999. Cellular distribution of the calcium-binding proteins parvalbumin, calbindin, and calretinin in the neocortex of mammals: phylogenetic and developmental patterns. J. Chem. Neuroanat. 16 (2), 77–116.
Hof, P.R., Lüth, H.J., Rogers, J.H., Celio, M.R., 1993. Calcium-binding proteins define subpopulations of interneurons in cingulate cortex. In: Vogt, B.A., Gabriel, M. (Eds.), Neurobiology of Cingulate Cortex and Limbic Thalamus: A Comprehensive Handbook. Birkhäuser, Basel, pp. 181–205.
Hof, P.R., Nimchinsky, E.A., 1992. Regional distribution of neurofilament and calcium-binding proteins in the cingulate cortex of the macaque monkey. Cereb. Cortex 2 (6), 456–467.
Hof, P.R., Nimchinsky, E.A., Perl, D.P., Erwin, J.M., 2001. An unusual population of pyramidal neurons in the anterior cingulate cortex of hominids contains the calcium-binding protein calretinin. Neurosci. Lett. 307, 139–142.
Hung, Y., Smith, M.L., Taylor, M.J., 2012. Development of ACC-amygdala activations in processing unattended fear. Neuroimage 60 (1), 545–552.
Kawaguchi, Y., Kondo, S., 2002. Parvalbumin, somatostatin, and cholecystokinin as chemical markers for specific GABAergic interneuron types in the rat prefrontal cortex. J. Neurocytol. 31 (3–5), 277–287.
Kawaguchi, Y., Kubota, Y., 1997. GABAergic cell subtypes and their synaptic connections in rat frontal cortex. Cereb. Cortex 7 (6), 476–486.
Leech, R., Sharp, D.J., 2014. The role of the posterior cingulate cortex in cognition and disease. Brain 137 (Pt 1), 12–32.
Legaz, I., Olmos, L., Real, M.A., Guirado, S., Dávila, J.C., Medina, L., 2005. Development of neurons and fibers containing calcium binding proteins in the pallial amygdala of mouse, with special emphasis on those of the basolateral amygdalar complex. J. Comp. Neurol. 488 (4), 492–513.
Levar, N., van Leeuwen, J.M.C., Puts, N.A.J., Denys, D., van Wingen, G.A., 2017. GABA concentrations in the anterior cingulate cortex are associated with fear network function and fear recovery in humans. Front. Hum. Neurosci. 11, 202, http://dx.doi.org/10.3389/fnhum.2017.00202.
Luzzati, F., Nato, G., Oboti, L., Vigna, E., Rolando, C., Armentano, M., Bonfanti, L., Fasolo, A., Peretto, P., 2014. Quiescent neuronal progenitors are activated in the juvenile guinea pig lateral striatum and give rise to transient neurons. Development 141 (21), 4065–4075.
Markram, H., Toledo-Rodriguez, M., Wang, Y., Gupta, A., Silberberg, G., Wu, C., Monyer, H., 2004. Interneurons of the neocortical inhibitory system. Nat. Rev. Neurosci. 5 (10), 793–807.
Mascagni, F., Muly, E.C., Rainnie, D.G., McDonald, A.J., 2009. Immunohistochemical characterization of parvalbumin-containing interneurons in the monkey basolateral amygdala. Neuroscience 158 (4), 1541–1550.
Mészár, Z., Girard, F., Saper, C.B., Celio, M.R., 2012. The lateral hypothalamic parvalbumin-immunoreactive (PV1) nucleus in rodents. J. Comp. Neurol. 520 (4), 798–815.
Miettinen, R., Sirviö, J., Riekkinen Sr., P., Laasko, M.P., Riekkinen, M., Riekkinen Jr., P., 1993. Neocortical, hippocampal and septal parvalbumin- and somatostatin-containing neurons in young and aged rats: correlation with passive avoidance and water maze performance. Neuroscience 53 (2), 367–378.
Moon, J.S., Kim, J.J., Chang, I.Y., Chung, Y.Y., Jun, J.Y., You, H.J., Yoon, S.P., 2002. Postnatal development of parvalbumin and calbindin D-28k immunoreactivities in the canine anterior cingulate cortex: transient expression in layer V pyramidal cells. Int. J. Dev. Neurosci. 20 (6), 511–519.
Moss, J., Toni, N., 2013. A circuit-based gatekeeper for adult neural stem cell proliferation: parvalbumin-expressing interneurons of the dentate gyrus control the activation and proliferation of quiescent adult neural stem cells. Bioessays 35 (1), 28–33.
Nimchinsky, E.A., Vogt, B.A., Morrison, J.H., Hof, P.R., 1997. Neurofilament and calcium-binding proteins in the human cingulate cortex. J. Comp. Neurol. 384 (4), 597–620.
Oblak, A.L., Rosene, D.L., Kemper, T.L., Bauman, M.L., Blatt, G.J., 2011. Altered posterior cingulate cortical cytoarchitecture, but normal density of neurons and interneurons in the posterior cingulate cortex and fusiform gyrus in autism. Autism Res. 4 (3), 200–211.
Papez, J.W., 1995. A proposed mechanism of emotion., 1937. A proposed mechanism of emotion. J. Neuropsychiatry Clin. Neurosci. 7 (1), 103–112.
Pearson, J.M., Heilbronner, S.R., Barack, D.L., Hayden, B.Y., Platt, M.L., 2011. Posterior cingulate cortex: adapting behavior to a changing world. Trends Cogn. Sci. 15 (4), 143–151.
Piantoni, G., Cheung, B.L., Van Veen, B.D., Romeijn, N., Riedner, B.A., Tononi, G., Van Der Werf, Y.D., Van Someren, E.J., 2013. Disrupted directed connectivity along the cingulate cortex determines vigilance after sleep deprivation. Neuroimage 79, 213–222.
Pitkänen, A., Amaral, D.G., 1993. Distribution of parvalbumin-immunoreactive cells and fibers in the monkey temporal lobe: the amygdaloid complex. J. Comp. Neurol. 331 (1), 14–36.
Pontes, A., Zhang, Y., Hu, W., 2013. Novel functions of GABA signaling in adult neurogenesis. Front. Biol. (Beijing) 8 (5), http://dx.doi.org/10.1007/s11515-013-1270-2.
Raghanti, M.A., Spocter, M.A., Butti, C., Hof, P.R., Sherwood, C.C., 2010. A comparative perspective on minicolumns and inhibitory GABAergic interneurons in the neocortex. Front. Neuroanat. 4, 3, http://dx.doi.org/10.3389/neuro.05.003.2010.
Raj, A., Kuceyeski, A., Weiner, M., 2012. A network diffusion model of disease progression in dementia. Neuron 73 (6), 1204–1215.
Robak, A., Szteyn, S., Bogus-Nowakowska, K., Równiak, M., 2003. The neuronal structure of the red nucleus in newborn guinea pigs. Folia Morphol. (Warsz) 62 (1), 1–9.
Równiak, M., Bogus-Nowakowska, K., Robak, A., 2015. The densities of calbindin and parvalbumin, but not calretinin neurons, are sexually dimorphic in the amygdala of the guinea pig. Brain Res. 1604, 84–97.
Schierle, G.S., Gander, J.C., D'Orlando, C., Ceilo, M.R., Vogt Weisenhorn, D.M., 1997. Calretinin-immunoreactivity during postnatal development of the rat isocortex: a qualitative and quantitative study. Cereb. Cortex 7 (2), 130–142.
Schwaller, B., Durussel, I., Jermann, D., Herrmann, B., Cox, J.A., 1997. Comparison of the Ca2+-binding properties of human recombinant calretinin-22k and calretinin. J. Biol. Chem. 272 (47), 29663–29671.
Shaw, J.C., Palliser, H.K., Dyson, R.M., Berry, M.J., Hirst, J.J., 2018. Disruptions to the cerebellar GABAergic system in juvenile guinea pigs following preterm birth. Int. J. Dev. Neurosci. 65, 1–10.
Shaw, P., Kabani, N.J., Lerch, J.P., Eckstrand, K., Lenroot, R., Gogtay, N., Greenstein, D., Clasen, L., Evans, A., Rapoport, J.L., Giedd, J.N., Wise, S.P., 2008. Neurodevelopmental trajectories of the human cerebral cortex. J. Neurosci. 28 (14), 3586–3594.
Silveri, M.M., Sneider, J.T., Crowley, D.J., Covell, M.J., Acharya, D., Rosso, I.M., Jensen, J.E., 2013. Frontal lobe γ-aminobutyric acid levels during adolescence: associations with impulsivity and response inhibition. Biol. Psychiatry 74 (4), 296–304.
Sohal, V.S., Zhang, F., Yizhar, O., Deisseroth, K., 2009. Parvalbumin neurons and gamma rhythms enhance cortical circuit performance. Nature 459 (7247), 698–702.
Sorvari, H., Soininen, H., Paljärvi, L., Karkola, K., Pitkänen, A., 1995. Distribution of parvalbumin-immunoreactive cells and fibers in the human amygdaloid complex. J. Comp. Neurol. 360 (2), 185–212.
Turner, C.P., Connell, J., Blackstone, K., Ringler, S.L., 2007. Loss of calcium and increased apoptosis within the same neuron. Brain Res. 1128 (1), 50–60.
Vann, S.D., Nelson, A.J., 2015. The mammillary bodies and memory: more than a hippocampal relay. Prog. Brain Res. 219, 163–185.
Verhage, M., Maia, A.S., Plomp, J.J., Brussaard, A.B., Heeroma, J.H., Vermeer, H., Toonen, R.F., Hammer, R.E., van den Berg, T.K., Missler, M., Geuze, H.J., Südhof, T.C., 2000. Synaptic assembly of the brain in the absence of neurotransmitter secretion. Science 287 (5454), 864–869.
Wang, C., Shimizu-Okabe, C., Watanabe, K., Okabe, A., Matsuzaki, H., Ogawa, T., Mori, N., Fukuda, A., Sato, K., 2002. Developmental changes in KCC1, KCC2, and NKCC1 mRNA expressions in the rat brain. Brain Res. 139, 59–66.
West, J.R., 1987. Fetal alcohol-induced brain damage and the problem of determining temporal vulnerability: a review. Alcohol Drug Res. 7 (5–6), 423–441.
Wewers, D., Kaiser, S., Sachser, N., 2003. Maternal separation in guinea-pigs: a study in behavioural endocrinology. Ethology 109 (5), 443–453.

Woodruff, A., Xu, Q., Anderson, S.A., Yuste, R., 2009. Depolarizing effect of neocortical chandelier neurons. Front. Neural Circuits 3, 15, http://dx.doi.org/10.3389/neuro.04.015.2009.

Woodruff, A.R., Sah, P., 2007. Networks of parvalbumin-positive interneurons in the basolateral amygdala. J. Neurosci. 27 (3), 553–563.

Workman, A.D., Charvet, C.J., Clancy, B., Darlington, R.B., Finlay, B.L., 2013. Modeling transformations of neurodevelopmental sequences across mammalian species. J. Neurosci. 33 (17), 7368–7383.

Wouterlood, F.G., van Denderen, J.C., van Haeften, T., Witter, M.P., 2000. Calretinin in the entorhinal cortex of the rat: distribution, morphology, ultrastructure of neurons, and co-localization with gamma-aminobutyric acid and parvalbumin. J. Comp. Neurol. 425 (2), 177–192.

Wree, A., Zilles, K., Schleicher, A., 1981. A quantitative approach to cytoarchitectonics. VII. The areal pattern of the cortex of the guinea pig. Anat. Embryol. (Berl.) 162 (1), 81–103.

Wu, D., Deng, H., Xiao, X., Zuo, Y., Sun, J., Wang, Z., 2017. Persistent neuronal activity in anterior cingulate cortex correlates with sustained attention in rats regardless of sensory modality. Sci. Rep. 7, 43101, http://dx.doi.org/10.1038/srep43101.

Xiong, K., Luo, D.W., Patrylo, P.R., Luo, X.G., Struble, R.G., Clough, R.W., Yan, X.X., 2008. Doublecortin-expressing cells are present in layer II across the adult guinea pig cerebral cortex: partial colocalization with mature interneuron markers. Exp. Neurol. 211 (1), 271–282.

Xu, L., Zhang, X.H., 2015. Distribution of D1 and D2-dopamine receptors in calcium-binding-protein expressing interneurons in rat anterior cingulate cortex. Sheng Li Xue Bao 67 (2), 163–172.

Yan, Y.H., Van Brederode, J.F., Hendrickson, A.E., 1995. Transient colocalization of calretinin, parvalbumin, and calbindin-D28k in developing visual cortex of monkey. J. Neurocytol. 24 (11), 825–837.

Zaitsev, A.V., Gonzalez-Burgos, G., Povysheva, N.V., Kröner, S., Lewis, D.A., Krimer, L.S., 2005. Localization of calcium-binding proteins in physiologically and morphologically characterized interneurons of monkey dorsolateral prefrontal cortex. Cereb. Cortex 15 (8), 1178–1186.

Zhang, H., Dai, R., Qin, P., Tang, W., Hu, J., Weng, X., Wu, X., Mao, Y., Wu, X., Northoff, G., 2017. Posterior cingulate cross-hemispheric functional connectivity predicts the level of consciousness in traumatic brain injury. Sci. Rep. 7 (1), 387, http://dx.doi.org/10.1038/s41598-017-00392-5.

Zhao, C., Eisinger, B., Gammie, S.C., 2013. Characterization of GABAergic neurons in the mouse lateral septum: a double fluorescence in situ hybridization and immunohistochemical study using tyramide signal amplification. PLoS One 8 (8), e73750, http://dx.doi.org/10.1371/journal.pone.0073750.

Zimmermann, L., Schwaller, B., 2002. Monoclonal antibodies recognizing epitopes of calretinin: dependence on Ca2+-binding status and differences in antigen accessibility in colon cancer cells. Cell Calcium 31 (1), 13–25.

Żakowski, W., Robak, A., 2013. Developmental changes of calretinin immunoreactivity in the anterior thalamic nuclei of the guinea pig. J. Chem. Neuroanat. 47, 28–34.